Nonequilibrium Sorption of Water in Polylactide

ARTICLE *in* MACROMOLECULES · SEPTEMBER 2012

Impact Factor: 5.8 · DOI: 10.1021/ma301484u

Macromolecules

Article

pubs.acs.org/Macromolecules

Nonequilibrium Sorption of Water in Polylactide

Eric M. Davis,[†] Matteo Minelli,[‡] Marco Giacinti Baschetti,[‡] Giulio C. Sarti,[‡] and Yossef A. Elabd*[,†]

[†]Department of Chemical and Biological Engineering, Drexel University, Philadelphia, Pennsylvania 19104, United States

[‡]Dipartimento di Ingegneria Chimica Mineraria e delle Tecnologie Ambientali (DICMA), Università di Bologna, 40131 Bologna, Italy

Supporting Information

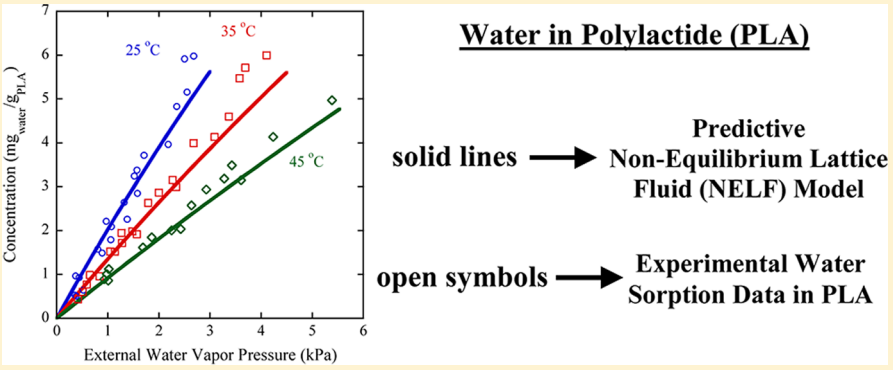

ABSTRACT: The sorption of water in polylactide (PLA) was measured at various vapor activities (0−0.85) and temperatures using a number of experimental techniques, including quartz spring microbalance (QSM), quartz crystal microbalance (QCM), and *in situ* time-resolved Fourier transform infrared-attenuated total reflectance (FTIR-ATR) spectroscopy. Additionally, a prediction of the water sorption isotherm in PLA was obtained with the use of the nonequilibrium lattice fluid (NELF) model, where an excellent agreement between the model prediction and experimental sorption data was observed at different experimental temperatures (all below the glass transition temperature of PLA) for water vapor activities less than 0.65. Results from *in situ* time-resolved FTIR-ATR spectroscopy revealed that water is present predominately as dimers in PLA at water vapor activities less than 0.65, and the presence of larger hydrogen-bound water clusters was observed at water vapor activities >0.65. This provides a rationale for the deviation between the NELF model prediction and water sorption data at high vapor activities, where the NELF model does not account for the strong self-association interactions present in large hydrogen-bound water clusters. Furthermore, non-Fickian sorption kinetic behavior was observed with all the experimental techniques, and this highlights the nonequilibrium nature of the water−glassy polymer system and provides insight into the variability in the sorption isotherms reported in the literature.

INTRODUCTION

Polylactide (PLA), a biodegradable polymer synthesized from renewable sources, is actively being pursued as a replacement to common commodity plastics synthesized from nonrenewable sources (e.g., poly(methyl methacrylate), poly(styrene), poly(ethylene terephthalate)).[1−3] Its comparable moisture barrier properties to materials, such as poly(methyl methacrylate), for example, may impact future products, such as medical implants and packaging.[1,4] Water sorption in PLA can vary substantially depending on the compositions of D- and L-isomers,[4,5] while there are conflicting reports on the effects of crystallinity on the moisture barrier properties of the material.[5−7] Therefore, an accurate assessment of water sorption and sorption kinetics (diffusion) in biodegradable glassy polymers is of great interest. More specifically, with few reports on water vapor sorption and diffusion in PLA,[4−7] a more accurate and fundamental investigation of water in PLA is warranted. Additionally, for the low water sorption values in PLA reported,[4,7] sensitive experimental techniques are required to accurately measure water sorption in glassy barrier polymers.

Recently, work by Davis et al.[8] highlighted the nonequilibrium nature of PLA when exposed to liquid water at room temperature, where both water diffusion and polymer relaxation (dilation due to water ingress) were observed to occur on similar time scales during the sorption process and were simultaneously measured with time-resolved Fourier transform infrared−attenuated total reflectance (FTIR-ATR) spectroscopy. With this coupled diffusion−relaxation phenomena, the water−PLA system deviates from true equilibrium, making it difficult to properly characterize moisture transport properties of this glassy material. Therefore, in order to accurately make comparisons and conclusions about reported experimental water sorption data, it must first be understood what sorption values are actually being measured and collected in these systems.

Received: July 17, 2012
Revised: August 31, 2012
Published: September 7, 2012

With regards to modeling the sorption of small molecules in glassy polymers, numerous research groups have adequately described sorption isotherms with the use of a simple Henry's law or Henry's law coupled with Langmuir sorption (i.e., dual-mode sorption model).[9−12] These models are useful in understanding the underlying sorption mechanisms but are not purely predictive and require multiple (up to three) fitting parameters. Additionally, the parameters for each penetrant−polymer system must be obtained at each temperature of interest, and the parameters for sorption and desorption must be different to account for hysteresis behavior.[12] These parameters have also been shown to be dependent on the pressure region used for fitting.[13] Ultimately, the use of a purely predictive model to represent the sorption behavior in glassy polymers can provide more insight into the physics underlying the sorption process.

Recently, Li et al.[14] have shown an adequate prediction of the sorption of noncondensable gases (CO_2 and N_2) in PLA with the use of both the Sanchez−Lacombe equation of state (SL-EoS) and Simha−Somcynsky equation of state (SS-EoS). One should note that this work was at temperatures well above the glass transition temperature of PLA and therefore describes the sorption behavior of PLA in its rubbery or equilibrium state. Even more recently, Kasturirangan et al.[15] have predicted sorption isotherms of CO_2 in PLA using a modified lattice model developed by Ozkan and Teja.[16] These predictions and sorption experiments were also at or above the glass transition temperature of PLA. Although the prediction of sorption in PLA above the glass transition temperature (equilibrium state) is useful, an adequate prediction below the glass transition temperature (e.g., at room temperature) or in its non-equilibrium state may be even more useful. Therefore, a model that incorporates nonequilibrium thermodynamics must be applied to understand sorption in a polymer that is in its glassy or pseudo-frozen state.

Doghieri and Sarti have developed such a model, known as the nonequilibrium lattice fluid (NELF) model,[12] which incorporates both the lattice fluid model developed by Sanchez and Lacombe[17] and nonequilibrium thermodynamics. The NELF model has been successfully employed to accurately predict the sorption of gases in glassy polymers.[12,18,19] In the NELF model, the constraints of equilibrium thermodynamics are relaxed by assigning the polymer density as an order parameter to account for the systems departure from equilibrium during the sorption process.

In this study, the NELF model was utilized to accurately predict the sorption of water vapor in a glassy polymer (PLA) at three separate temperatures, all below the glass transition temperature of the polymer. These predictions were compared with experimental gravimetric data obtained from two separate techniques, quartz spring microbalance (QSM), and quartz crystal microbalance (QCM), where excellent agreement between the model and experimental data was observed up to a water vapor activity of 0.65. Additionally, the states of water in the PLA film were investigated with the use of *in situ* time-resolved FTIR-ATR spectroscopy. This technique provides molecular-level contrast between the penetrant (e.g., water) and the polymer in real time. It also provides molecular-level information about the distribution of the states of water and water transport mechanisms, which offers key insight into guiding thermodynamic modeling of the water−glassy polymer system.

EXPERIMENTAL SECTION

Materials. Polylactide (PLA) (M_w = 140 600 g/mol, PDI = 2.27, T_g = 57 °C) was purchased from Nature Works LLC in pellet form (PLA 4060D, a racemic mixture of D/L-isomers); the chemical structure is shown in Figure 1. The molecular weight of the PLA was determined

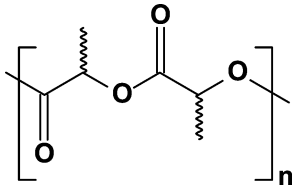

Figure 1. Chemical structure of polylactide (PLA).

using gel permeation chromatography (GPC) at 40 °C using a Waters GPC system (breeze 1) equipped with 1 Styragel column and a 2414 refractive index (RI) detector (see Supporting Information, Figure S1). GPC measurements were performed at a flow rate of 1.0 mL/min at 40 °C using poly(styrene) (PS) as a standard. The T_g and completely amorphous nature of PLA 4060D were measured and confirmed by differential scanning calorimetry (DSC) (see Figure S2). Thermograms were measured with a TA Instruments Q200 DSC over a temperature range of −10 to 205 °C at a heating rate of 10 °C/min under a nitrogen environment. Chloroform (99.8% purity; ACS reagent) was purchased from Aldrich. Double distilled deionized water (conductivity = 0.01 μS/cm) was used for all sorption experiments.

Film Preparation. PLA/chloroform solutions were prepared by dissolving PLA pellets in chloroform at 5% w/w and mixing for 24 h to ensure a clear, homogeneous solution. PLA film fabrication consisted of solution casting the PLA/chloroform solution onto a Teflon Petri dish to produce free-standing films for QSM experiments or solution casting directly onto the ATR crystal surface for time-resolved FTIR-ATR spectroscopy experiments. For both QSM and ATR experiments, the polymer solution was dried in ambient conditions for 24 h after deposition. This was followed by annealing the film at 70 °C under vacuum for 3 h. For QCM experiments, PLA films were spun-coat unto a gold QCM crystal (15 s at 900 rpm, followed by 15 s at 1500 rpm). Before annealing, the stability of the PLA-coated QCM crystals was evaluated (i.e., the frequency of the coated crystal was monitored over time). If the baseline frequency drift of the coated crystal was too large, the coated crystal was then placed back in the spin coater and exposed to a drop of pure chloroform at 1000 rpm. This was then followed by the aforementioned annealing protocol. After film fabrication, all PLA films were immediately stored in a desiccator prior to all sorption experiments. Immediately following each experiment, the thickness of the PLA films for QSM and ATR experiments was measured using a digital micrometer (Mitutoyo) with a 1 μm accuracy. Each film thickness was an average of at least three individual measurements at different positions along the length of the film. Average film thicknesses for the QSM, QCM, and ATR experiments were ca. 80−150, 7, and 90 μm, respectively. The film thickness for QCM experiments was estimated from the measured polymer mass, the electrode area, and the polymer density (1.24 g/cm^3).

Quartz Spring Microbalance (QSM). A PLA film (ca. 50 mg), along with metal reference (ca. 20 mg), was placed at the end of a vertical quartz spring (purchased from DeerSlayer Springs; 100 mg maximum load with 500 mm maximum extension; spring constant, k_{spring} = 0.98 g/s^2), which was housed inside a temperature-controlled glass column. The glass column, along with a temperature-controlled reservoir,[20] was completely evacuated of moisture and air via vacuum for at least 2 h. After the system was completely evacuated, the valve connecting the glass column (housing the quartz spring and sample) to the rest of the experimental apparatus was closed (leak rate less than 0.2 mmHg/day). The reservoir containing deionized water was subjected to a number of freeze−thaw vacuum cycles in order to remove all dissolved gases from the liquid. Pure water vapor was then

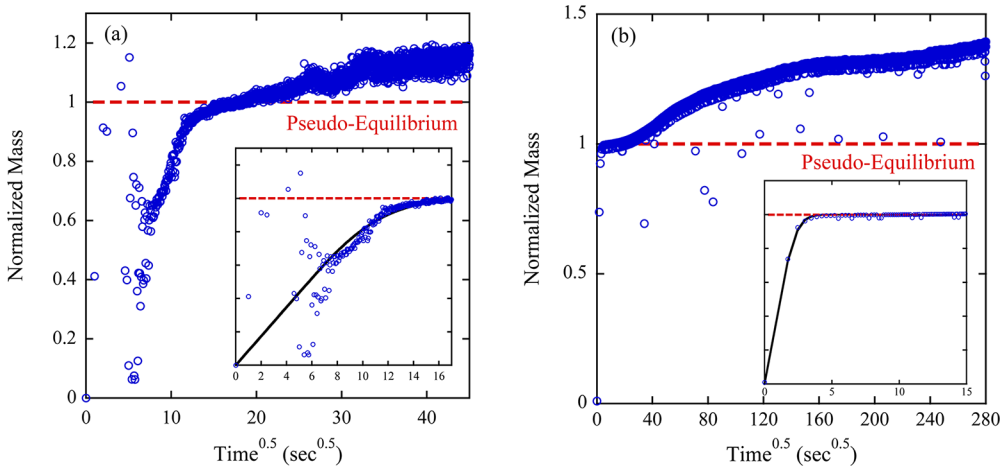

Figure 2. Water sorption kinetics in PLA at 35 °C measured with (a) QSM and (b) QCM. The sorption kinetic data were collected in response to an external differential change in water vapor activity of 0.53−0.65 and 0.45−0.69 for the QSM and QCM experiments, respectively. The insets correspond to a magnified view of the early time data, where solid lines correspond to a regression to the solution to Fick's second law (eq 1). The dashed lines correspond to pseudo-equilibrium values, where the measured sorption values were determined.

charged into the temperature-controlled reservoir at specific partial pressures, where it was allowed to equilibrate with the temperature of the jacket until steady state was reached (i.e., the pressure transducer reading was constant). Once steady state was reached, the valve separating the reservoir from the glass column was fully opened, exposing the PLA film in the glass column to a specified partial pressure of water. The change in the extension of the spring due to water sorbing into the polymer was measured as a function of time with a high-speed charge coupled device (CCD) camera (DVT SmartImage Sensor Series 600 Model 630). The mass of water sorbed in PLA was calculated from this spring extension data with the use of the spring constant and a force balance (i.e., $F = mg = kx$). The calculated minimum measurable change in mass that can be recorded is ca. 0.2 mg_{water}/g_{PLA} based on the resolution of the CCD camera and spring constant. The water diffusion coefficient can be obtained from regressing the experimental data (mass versus time) to the solution of Fick's second law with the appropriate boundary and initial conditions:[21]

$$\frac{M(t)}{M(\infty)} = 1 - \sum_{n=0}^{\infty} \frac{8}{(2n+1)^2\pi^2} \exp\left(\frac{-D(2n+1)^2\pi^2 t}{4L^2}\right) \quad (1)$$

where $M(t)$ and $M(\infty)$ are the mass at time t and at long times, respectively, and the diffusion coefficient, D, is the only adjustable parameter. More details about this apparatus and procedures can be found elsewhere.[20]

Quartz Crystal Microbalance (QCM). The entire QCM apparatus (purchased from Elbatech, Italy), including sample chamber and water reservoir, was enclosed and sealed in a metal tank and completely submerged in a temperature-controlled bath, where water vapor at specific partial pressures was charged into the sample chamber. The QCM measures the frequency shift of a 9 MHz AT cut quartz crystal (purchased from Kyushu Dentsu Co., Ltd., Japan). Raw frequency values were converted to actual mass uptake in the PLA film through the use of the Sauerbrey equation:[22]

$$\Delta f = \left[\frac{-2f_0^{\,2}}{A\sqrt{\rho_Q G_Q}}\right]\Delta m \quad (2)$$

where Δf is the change in frequency to due to the addition of sorbed mass, f_0 is the resonance frequency of the bare oscillator, A is the surface area of the coated crystal, and ρ_Q and G_Q are the density and shear modulus of the quartz, respectively. More details regarding the experimental apparatus and experimental procedures can be found elsewhere.[23]

Optical Micrometer. Polymer swelling (dilation) experiments were performed using an optical micrometer apparatus. The sample chamber is comprised of a stainless steel cell with two borosilicate glass windows on either side, allowing optical access for swelling measurements. The stainless steel cell is connected to a penetrant reservoir with pressure transducer, allowing for different partial pressures of penetrant to be charged into the sample cell. The sensing element is an optical micrometer (Keyence LS-7030-M) equipped with a high-speed, linear charge-coupled device (CCD) sensor with an accuracy of 1 μm and reproducibility within 0.15 μm in the measurements. To control the temperature, heating tape surrounded the sample cell and the penetrant reservoir and was housed on a heating plate. More details regarding the experimental apparatus can be found elsewhere.[24,25]

Time-Resolved FTIR-ATR Spectroscopy. Water sorption was also measured with time-resolved infrared spectroscopy using an FTIR spectrometer (Nicolet 6700 Series; Thermo Electron) equipped with a horizontal, temperature-controlled ATR cell (Specac Inc.). The PLA films were deposited on a multiple reflection, trapezoidal zinc selenide ATR crystal (Specac Inc.) with 45° beveled faces. All spectra were collected using a liquid nitrogen-cooled mercury−cadmium−telluride (MCT) detector with 32 scans per spectrum at a resolution of 2 cm^{-1}, where a spectrum was collected every 15 s. Transport experiments were conducted at 25, 35, and 45 °C, controlled by a temperature jacket (circulated water bath) on the ATR flow through cell. The ATR flow through cell was connected directly to the vapor sorption apparatus.

Before each transport experiment, a background spectrum of the bare ATR crystal was collected, and all subsequent collected spectra were subtracted from this spectrum. Then, a PLA-coated ATR crystal was mounted into the ATR flow through cell with a Kalrez gasket, and the cell was sealed. The reservoir in the vapor sorption apparatus contained pure liquid water and was pretreated with multiple freeze−thaw−vacuum cycles in order to ensure complete removal of any dissolved gases from the water.

To begin each transport experiment, the vapor sorption/ATR combined system was evacuated for at least 2 h prior to the start of each experiment (i.e., pressure transducer reached constant value). Then pure water vapor was charged into the vapor sorption system at a specific partial pressure and allowed to equilibrate (i.e., the pressure transducer reading was constant). Once this equilibrium was reached, the valve separating the ATR cell from the rest of the system was opened, allowing pure water vapor to enter the ATR cell in the space (V = 550 μL) above the polymer film (the side opposite the polymer−crystal interface). This was followed by the collection of time-resolved

dx.doi.org/10.1021/ma301484u | Macromolecules 2012, 45, 7486−7494

infrared spectra. More details regarding the apparatus and experimental procedures can be found elsewhere.[26]

RESULTS AND DISCUSSION

Experimental Water Sorption in PLA. Figure 2 shows the water sorption kinetics in PLA at 35 °C, after a differential change of the external water activity, for both QSM and QCM. It is clear that for both techniques the sorption kinetics exhibit non-Fickian or anomalous behavior. Similar non-Fickian or anomalous sorption has been previously observed using gravimetric techniques,[27] where this behavior has been attributed to diffusion and polymer relaxation occurring on different time scales in a nonequilibrium glassy polymer during reasonable experimental time scales.[21,28] The insets in Figure 2a,b show that Fickian-like behavior was observed in both the QSM and QCM data over an initial short time scale, with the remarkable feature that for both cases the same Fickian diffusivity (ca. 1×10^{-7} cm^2/s) was obtained, within experimental errors. Furthermore, the data in Figure 2 were normalized to the mass at the Fickian pseudo-equilibrium value to help distinguish between these two phenomena (diffusion and relaxation), which occur over two distinct time periods over the entire experimental time. The insets in Figure 2 illustrate the first period, where Fickian-like or pseudo-Fickian behavior can be clearly seen, where the pseudo-equilibrium normalization allows for a simple regression of the Fickian diffusion coefficient for the first period of the data. However, at longer times, the nonequilibrium state of the glassy polymer relaxes and allows more water to enter into the polymer gradually over this dwelling time.

This is an important experimental feature where great care must be taken when collecting data because if the time scales of the experiments are too short (with respect to the relaxation time of the polymer) or the polymer films are too thick (i.e., the characteristic time for diffusion is longer than relaxation time), this anomalous behavior could not be clearly observed, and the sorption behavior would appear Fickian-like. It is worth reminding, as indicated in the Experimental Section, that the PLA film thicknesses were different between the QSM (~130 μm) and QCM (~7 μm) experiments due to the different experimental procedures, where QSM requires solution-cast free-standing films and QCM requires spun-cast films on a quartz crystal substrate. As a consequence, the time scale for Fickian-like behavior is much smaller in the QCM experiments compared to those in QSM, where sorption data reach a Fickian pseudo-equilibrium value in ca. 3 $s^{1/2}$ (9 s) and ca. 15 $s^{1/2}$ (225 s) in QCM and QSM experiments, respectively. The experimental times for each experiment were extended to adequately observe the subsequent anomalous diffusion–relaxation behavior and point out its importance in the evaluation of meaningful and reliable solubility values for this kind of system. The samples used in QCM apparatus have a mechanical constraint to deformation, not present in QSM samples. That can affect the relaxation behavior and would require a separate analysis. Therefore, in order to use a consistent reference for the comparison between the different experimental techniques in this work, the sorption values reported for both techniques were taken from the pseudo-equilibrium state of the kinetic data (the plateau reached after Fickian diffusion with the same diffusivity) shown by the dashed lines in Figure 2. However, on the basis of data shown in Figure 2, one could report an infinite number of sorption values after the pseudo-equilibrium time, depending on the length of the experiment. This highlights that the actual sorption values reported here, or by any other experimental report, reflect in fact not a true equilibrium property, but rather the nonequilibrium sorption of water in a glassy polymer. This also provides a rationale for the differences among reports on water solubility in PLA, where these reports do not specify at what experimental time they extract their sorption values. This may also be the reason why the water sorption values in this work are slightly lower than those previously reported,[4,7] while matching quite well with other reports.[29]

In Figure 2a, the noise in the early time data is a result of the buoyancy of the quartz spring, where the spring and sample oscillate in a decaying, periodic fashion as a result of the sudden change in external water vapor pressure due to the differential step change introduced. Depending on the thickness and weight of the sample, this oscillation and subsequent noise in the water sorption kinetics can vary.

The sorption isotherms of water in PLA, experimentally measured with the use of both QSM and QCM, are shown in Figures 3 and 4. Figure 3 shows sorption isotherms of water in PLA at three different temperatures, 25, 35, and 45 °C, measured by QSM and plotted as a function of external water

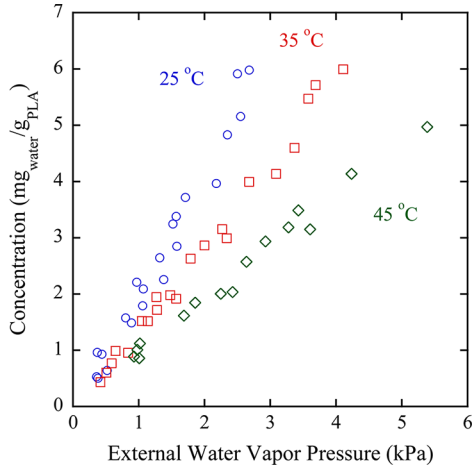

Figure 3. Sorption isotherms of water in PLA measured with QSM at 25, 35, and 45 °C plotted versus external water vapor partial pressure.

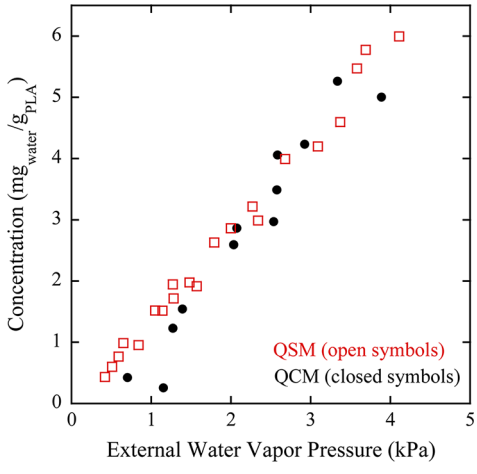

Figure 4. Comparison of sorption isotherms of water in PLA measured by both QSM and QCM at 35 °C.

dx.doi.org/10.1021/ma301484u | Macromolecules 2012, 45, 7486–7494

vapor partial pressure. The data were collected over a wide range of water vapor activity (partial pressure normalized by saturation pressure), between 0.08 and 0.85; correspondingly, measured water solubilities in PLA spanned between 0.4 and 6.1 mg_{water}/g_{PLA}.

For comparison, water sorption in PLA was also measured with QCM. Figure 4 compares these QCM data with the previous QSM data at 35 °C. Over a broad water vapor activity range, it is clear that the water sorption data obtained from both techniques are in good agreement with one another.

Nonequilibrium Thermodynamic Prediction of Water Sorption in PLA. In order to predict the sorption isotherms of water in PLA, a nonequilibrium lattice fluid (NELF) model was employed. Details regarding this model can be found elsewhere.[12,19] A summary of the model used here, which utilizes the Sanchez–Lacombe equation of state (SL-EoS), is also given in the Supporting Information as further reference. The NELF model has been successfully used in previous work to predict the solubility of noncondensable gases in glassy polymers,[18,30] and more recently, this model has been extended to the prediction of condensable vapors[31] and liquids[32] in glassy polymers. The NELF model predicts sorption based on pure component data; therefore, the first step for its purely predictive use is to obtain the pure component parameters for both the polymer (PLA) and the penetrant (water). The SL pure component parameters (T^*, P^*, and ρ^*) for the polymer and penetrant are obtained by fitting the pure component data with the SL-EoS; in the present case, PvT data were used for PLA, while for water existing literature values were considered, obtained by fitting vapor pressure and saturated liquid density PvT data.[34]

Figure 5 shows an adequate regression of the PLA PvT data to the SL-EoS above the glass transition temperature of the polymer. Table 1 lists the SL pure component parameters that were determined for PLA (from Figure 5) and water (from ref 34). Although the SL-EoS does not account for strong association interactions between molecules, such as the self-association (hydrogen-bonding) of water, the use of SL-EoS was still pursued in this work; these strong molecular interactions, indeed, are likely not relevant in view of the very low solubility of water in the PLA (<1 wt %). A model that incorporates strong association interactions, such as statistical associating fluid theory (SAFT),[35] would introduce two additional parameters, which will extend the overall number of pure component parameters to five. Furthermore, recently, it has been shown that the NELF model is appropriate to calculate the low solubility values of vapor and liquid water in bisphenol A polycarbonate and in polysulfone.[32]

In addition to obtaining the SL pure component parameters, the swelling coefficient (k) and binary interaction parameter (K_{12}) must be obtained to provide an accurate sorption prediction. The first one accounts for the dilation of the polymer (change in polymer density) during sorption, and the latter characterizes the energetic interactions and their deviation from the geometric mean rule. To obtain a swelling coefficient, a separate dilation experiment was performed, where the volume change of the polymer was measured in response to exposure to water vapor. This is important because the polymer is below its glass transition temperature and therefore in a nonequilibrium state. In other words, its volume change when exposed to small molecule sorption does not follow the usual relationship of equilibrium thermodynamics, and in general it is not predictable a priori through the use of an equation of state. Therefore, the nonequilibrium volumetric behavior of the PLA–water mixture must be measured to accurately account for the nonequilibrium thermodynamics of this system. Figure 6 shows the results from a dilation experiment, where a dry PLA film was exposed to a sudden change in water vapor activity (i.e., integral sorption step) from 0 to 0.55 (the highest obtainable external water pressure for this experiment), and the change in volume of the PLA film was measured with an optical micrometer coupled with a high-

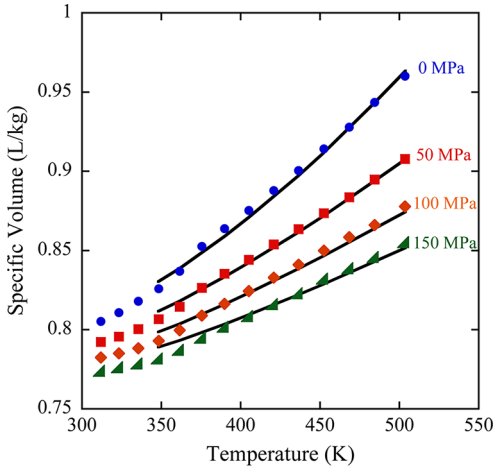

Figure 5. PvT data for PLA[33] used for the calculation of SL-EoS parameters. Solid lines represent the regressed SL-EoS.

Table 1. Pure Component SL Parameters for PLA and H_2O

parameters	PLA	H_2O[a]
T^* (K)	600	670
P^* (MPa)	600	2400
ρ^* (kg/L)	1.34	1.050

[a]Pure component parameters obtained from ref 34.

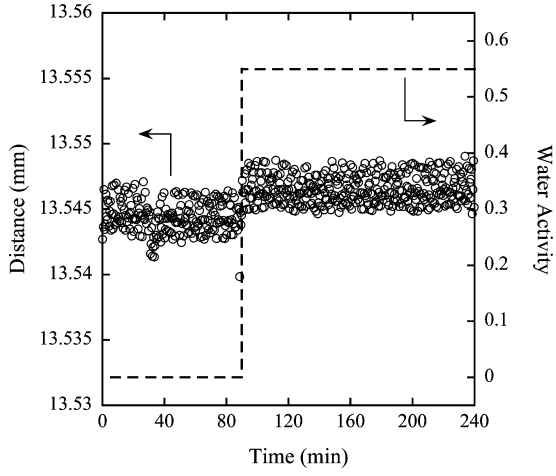

Figure 6. Dilation experiment at 35 °C: PLA film exposed to a sudden change in water vapor activity from 0 to 0.55, where volume change was measured by a change in length of the PLA film with an optical micrometer equipped with a high-speed CCD camera. Dashed line represents the change in water activity, i.e., sudden change in water vapor pressure.

dx.doi.org/10.1021/ma301484u | Macromolecules 2012, 45, 7486–7494

speed CCD camera. Dilation measurements were performed over a time interval longer than the time required to reach the Fickian plateau.

Polymer dilation was determined by measuring the distance between two reference points marked on the PLA film. The change in distance between these two reference points could then be used to calculate volume swelling of the polymer film: the one-dimensional length change was converted into three-dimensional dilation (volume change) assuming isotropic swelling. The dashed line in Figure 6 represents the measure of water vapor activity in the sample chamber housing the polymer film. The swelling coefficient (k) of the polymer is a material specific parameter and represents how the density (polymer volume) changes as a function of water activity (or external water pressure). If a polymer noticeably swells during the sorption process, then a measurable volume change (or decrease polymer density) will be observed. From analysis of the experimental data presented in Figure 6, it was determined that the observed polymer dilation (<0.02%) was less than the error associated with the experiment (ca. 0.04%), indicating there was no measurable swelling observed during the water sorption process, neither at the shorter times where relaxation is not yet effective nor in the subsequent postperiod inspected. Therefore, for the NELF model, a value of $k = 0$ was assumed, which parallels what was observed for the case of water sorption in polycarbonate and in polysulfone.[32]

The last information required for the NELF model prediction is the binary interaction parameter, K_{12}, associated with the penetrant−polymer binary mixture, which can be independently determined by regressing water sorption data of the polymer in its equilibrium state (i.e., above the glass transition temperature). Under those conditions, the equilibrium EoS can be employed to predict the volumetric behavior of the PLA−water mixture. Above T_g, therefore, solubility in the polymer is solely determined by the interaction between polymer and penetrant. Figure 7 shows the experimental water sorption isotherm in PLA at 65 °C (ca. 10 °C above the T_g of PLA), where the binary interaction parameter $K_{12} = -0.005$ was obtained from a regression to the SL-EoS or equilibrium lattice fluid model.

With the known values of SL pure component parameters (T^*, P^*, ρ^*), swelling coefficient ($k = 0$), and binary interaction parameter ($K_{12} = -0.005$), all obtained independently, the NELF model can be employed to provide a purely predictive water sorption isotherm at any given temperature. Figure 8 shows the NELF model predictions for sorption isotherms of water in amorphous PLA at 25, 35, and 45 °C, where these predictions are overlaid with experimentally obtained data shown previously (Figure 3).

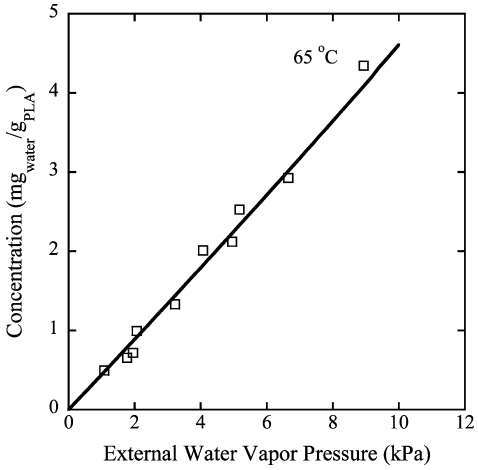

Figure 7. Water sorption isotherm in PLA at 65 °C (ca. 10 °C above T_g of PLA). Solid line represents equilibrium LF model regression with the interaction parameter (K_{12}) as the only adjustable parameter.

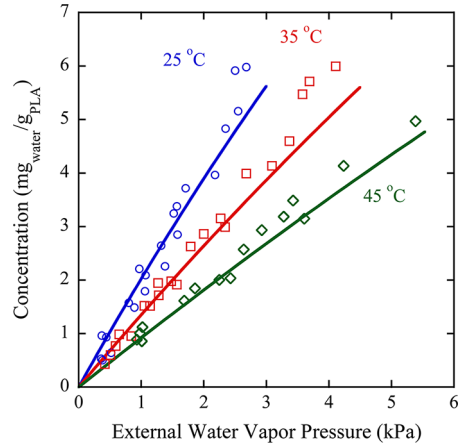

Figure 8. NELF model predictions (solid lines) of sorption isotherms of water in amorphous PLA as a function of external water pressure at 25, 35, and 45 °C. Open symbols represent experimental data obtained using QSM.

Remarkably, there is good agreement between the NELF model prediction and the experimental water sorption isotherms at all three temperatures. This finding is extremely interesting and somewhat surprising. Unlike the SAFT[35] and PC-SAFT[36] equations of state, the SL-EoS does not account for strong association interactions between molecules, e.g., self-association of water due to hydrogen bonding. Therefore, one would expect that the SL-EoS would poorly describe any binary system that includes water as one of the components, if strong hydrogen bonding is relevant. However, the accurate description of the equilibrium solubility isotherm of water at 65 °C in PLA, up to ca. 4 mg_{water}/g_{PLA}, with the use of the equilibrium SL EoS, as well as the accurate prediction with the NELF model below T_g can both be explained by the low values of water sorption in PLA at all vapor pressures. In other words, this finding suggests that the systems in this study are close to the infinite dilution limit, where the self-association or clustering of water molecules does not play a significant role. It should also be noted that while the NELF prediction at 45 °C is in good agreement with the experimental data over the entire activity range explored, there is a slight deviation between the NELF prediction and the experimental data at 25 and 35 °C at water vapor activities above ca. 0.65, corresponding to a concentration of water in the polymer of ca. 5 mg_{water}/g_{PLA}.

Deviation between Experimental Data and Model Predictions: States of Water. At 25 and 35 °C above a water vapor activity of ca. 0.65, some deviation between the NELF model prediction and experimental sorption data is visible. This deviation might be due, in principle, to polymer dilation or self-association of water molecules (i.e., water clusters) that may be present at water sorption values larger than 5 mg_{water}/g_{PLA}, encountered at these elevated water vapor activities. However, no measurable dilation was observed up to a water vapor

dx.doi.org/10.1021/ma301484u | Macromolecules 2012, 45, 7486−7494

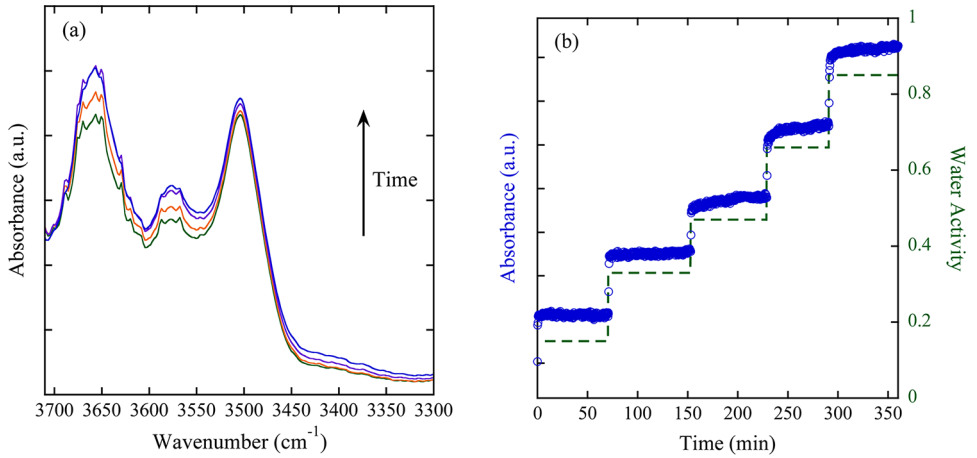

Figure 9. Time-resolved FTIR-ATR spectroscopy data of water vapor diffusion in PLA at 35 °C: (a) Time-resolved infrared absorbance of O−H stretching region (water) after exposure to a differential water vapor activity step from 0.47 to 0.66. (b) Integrated infrared absorbance (3575 cm^{-1}; water dimer) as a function of time in response to multiple differential water vapor activity steps.

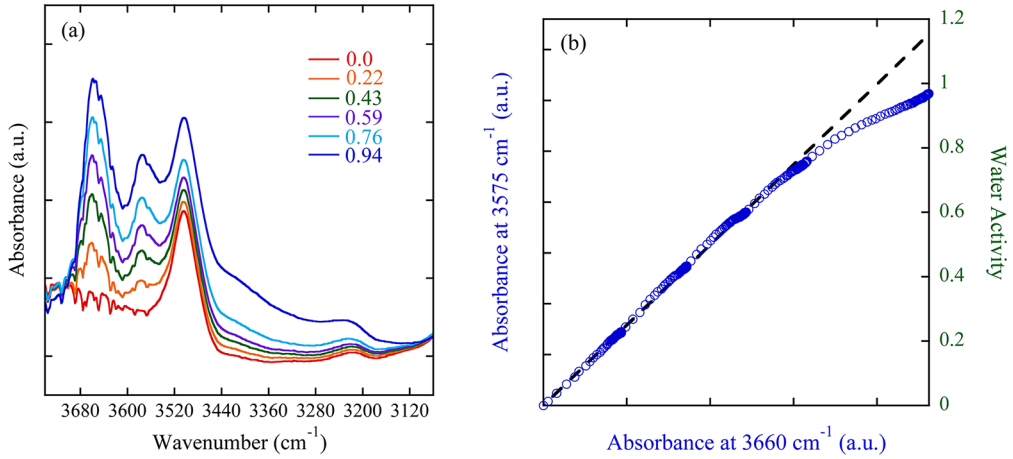

Figure 10. FTIR-ATR spectroscopy data of water in PLA at 35 °C: (a) O−H stretching infrared absorbance data at pseudo-equilibrium values after exposure to several differential water vapor activity steps (numbers on graph); (b) integrated, time-resolved water O−H stretching infrared absorbance (open circles) associated with the free O−H and dimer hydrogen-bound O−H plotted against each other over the entire length of the sorption experiment. Dashed line corresponds to 45° line.

activity of 0.55 so that polymer swelling seems not likely to be the reason for the observed deviation, making self-association of water molecules the more plausible option. At higher water vapor activities and water sorption values, the density of water molecules in PLA increases, and therefore the likelihood of self-association may increase. To provide further insight into the states of water in PLA, time-resolved FTIR-ATR spectroscopy was employed over the entire water vapor activity range studied.

Differential water sorption experiments (i.e., small step changes in water vapor activity) were performed at 25, 35, and 45 °C with time-resolved FTIR-ATR spectroscopy to complement the QSM and QCM experiments. Figure 9a shows the time-resolved mid-infrared spectra of the O−H stretching region for water in PLA at 35 °C, in response to a single differential water vapor activity step (from 0.47 to 0.66). In response to this change in water vapor activity, water diffuses into the PLA film, resulting in an intensity increase with time of the infrared bands characteristic of water, as shown in Figure 9a. Figure 9b shows the integrated O−H stretching absorbance as a function of time in the PLA film due to water sorption in the polymer in response to exposure to multiple differential water activity steps at 35 °C.

In order to obtain a better understanding of the states of water present in PLA, the infrared spectra of the O−H stretching region of water was investigated at each pseudo-equilibrium state (Fickian plateau) after exposure to each differential water vapor step, as shown in Figure 10.

As seen in Figure 10a, three prominent infrared bands are present in the O−H stretching region. In Figure 10a, the band located at 3505 cm^{-1} is associated with the −OH end group in PLA.[8] The two bands located at 3575 and 3660 cm^{-1} can be attributed to two particular modes of water O−H stretching: the hydrogen-bonded O−H stretching of the dimer[37,38] and the free O−H stretching,[39,40] respectively. There is also a broader infrared band located between 3440 and 3280 cm^{-1}, which begins to increase in intensity above a water activity of ca. 0.59 but becomes clearly apparent at a water vapor activity above ca. 0.76. This band is representative of stronger hydrogen-bound O−H stretching associated with larger water clusters.[37]

Figure 10b shows a plot of the hydrogen-bound O−H dimer band at 3575 cm^{-1} versus the free O−H band at 3660 cm^{-1} over the entire sorption experiment. Below a water vapor

dx.doi.org/10.1021/ma301484u | Macromolecules 2012, 45, 7486−7494

activity of ca. 0.65, a linear relationship between the increase of these two bands can be observed. This suggests that both bands represent O−H bonds on the same molecule, i.e., the hydrogen-bound and free O−H of the water dimer, and therefore at water vapor activities <0.65, water predominately exists in PLA as dimers. Additionally, at water vapor activities above 0.65, a deviation from linearity is observed in Figure 10b. This deviation suggests that the two bands are no longer representative of the same water molecule or state of water. In other words, as the water vapor activity increases, larger clusters of water are also present at higher concentrations of water in PLA, and therefore the free O−H band at 3660 cm^{-1} represents not only the dimer but also higher water cluster sizes, e.g., hexamers.[41] This deviation at water vapor activities >0.65 also corresponds to the appearance of a broader infrared band located between 3440 and 3280 cm^{-1} shown in Figure 10a, which represents hydrogen-bound O−H stretching vibrations of larger water clusters. The observation of water clusters in PLA above these water vapor activities is consistent with clustering calculations (i.e., Zimm−Lundberg's theory) preformed previously,[29] where the presence of water clusters was suggested to occur in PLA above water vapor activities of ca. 0.5.

The above infrared spectroscopy results showing the states of water in PLA, specifically that water exists predominately as dimers at water vapor activities <0.65 and that larger water clusters are present at water vapor activities >0.65, corroborate with the deviation in the NELF model predictions at water vapor activities >0.65 (Figure 8). These results are also consistent with the fact that the NELF model does not account for the strong self-association interactions present with such penetrants as water. However, it is noteworthy that the NELF model provides an excellent prediction of water in PLA at low sorption values (<5 mg_{water}/g_{PLA}), where the state of water is predominantly dimers, whose behavior in the mixture is well described by a single binary interaction parameter.

CONCLUSIONS

This work demonstrates the ability of nonequilibrium thermodynamics (NELF model) to accurately predict sorption of water in PLA below its glass transition temperature. Specifically, the NELF model prediction of the sorption isotherm was in excellent agreement with gravimetric sorption data obtained from both QSM and QCM at 25, 35, and 45 °C (all temperatures below the glass transition temperature of PLA) for water vapor activities less than 0.65, while some deviations were observed at higher activities where the water sorption values exceeded ca. 5 mg_{water}/g_{PLA}. Detailed insights into the deviation between the model and data at activities greater than 0.65 were provided by *in situ* time-resolved FTIR-ATR spectroscopy data, which showed that water in PLA is primarily in dimer form at activities less than 0.65, while larger water clusters were observed at activities above 0.65. This provides a rationale for the deviation between model and data at activities above 0.65, where the NELF model does not account for the strong self-association interactions present in water. Interestingly, the NELF model does accurately predict water sorption in PLA over a large vapor activity range where hydrogen-bound water (dimers) is present in the polymer.

It is also important to note that in all cases the sorption kinetics showed an initial Fickian behavior, ending in a pseudo-equilibrium plateau, followed by a subsequent non-Fickian sorption dominated by a slow relaxation process in the polymer allowing for a slow gradual increase in water sorption over a longer time range. In this work, the pseudo-equilibrium value after Fickian sorption was recognized as a consistent reference to compare the pseudo-equilibrium sorption values obtained from the different techniques used. However, one could report an infinite number of sorption values after this time point. This can explain the variability among reported values of water solubility in PLA, where these reports do not specify at what experimental time they extract their sorption values nor the relation between time range and polymer film thickness.

ASSOCIATED CONTENT

Supporting Information

GPC and DSC data and a summary of the NELF model derivation. This material is available free of charge via the Internet at http://pubs.acs.org.

AUTHOR INFORMATION

Corresponding Author

*E-mail: elabd@drexel.edu.

Notes

The authors declare no competing financial interest.

ACKNOWLEDGMENTS

The authors acknowledge the financial support of the National Science Foundation (CAREER 0644593) and the United States Department of Agriculture and the United States Department of Energy (06GO96002).

REFERENCES

(1) Auras, R.; Harte, B.; Selke, S. *Macromol. Biosci.* **2004**, *4*, 835−864.
(2) Sinclair, R. G. *J. Macromol. Sci., Part A: Pure Appl. Chem.* **1996**, *5*, 585−597.
(3) Williams, C. K.; Hillmyer, M. A. *Polym. Rev.* **2008**, *48*, 1−10.
(4) Oliveira, N. S.; Gonçalves, C. M.; Coutinho, J. A. P.; Ferreira, A.; Dorgan, J.; Marrucho, I. M. *Fluid Phase Equilib.* **2006**, *250*, 116−124.
(5) Siparsky, G. L.; Voorhees, K. J.; Dorgan, J. R.; Schilling, K. J. *J. Environ. Polym. Degrad.* **1997**, *5*, 125−136.
(6) Drieskens, M.; Peeters, R.; Mullens, J.; Franco, D.; Lemstra, P. J.; Hristova-Bogaerds, D. G. *J. Polym. Sci., Part B: Polym. Phys.* **2009**, *47*, 2247−2258.
(7) Cairncross, R. A.; Ramaswamy, S.; O'Connor, R. *Int. Polym. Process.* **2007**, *22*, 33−37.
(8) Davis, E. M.; Theryo, G.; Hillmyer, M. A.; Cairncross, R. A.; Elabd, Y. A. *ACS Appl. Mater. Interfaces* **2011**, *3*, 3997−4006.
(9) Fredrickson, G. H.; Helfand, E. *Macromolecules* **1985**, *18*, 2201−2207.
(10) Huvard, G. S.; Stannett, V. T.; Koros, W. J.; Hopfenberg, H. B. *J. Membr. Sci.* **1980**, *6*, 185−201.
(11) Paul, D. R.; Koros, W. J. *J. Polym. Sci., Part B: Polym. Phys.* **1976**, *14*, 675−685.
(12) Doghieri, F.; Sarti, G. *Macromolecules* **1996**, *29*, 7885−7896.
(13) Bondar, V. I.; Kamiya, Y.; Yampol'skii, Y. P. *J. Phys. Chem. B* **1996**, *34*, 369−378.
(14) Li, G.; Li, H.; Turng, L. S.; Gong, S.; Zhang, C. *Fluid Phase Equilib.* **2006**, *246*, 158−166.
(15) Kasturirangan, A.; Grant, C.; Teja, A. S. *Ind. Eng. Chem. Res.* **2008**, *47*, 645−649.
(16) Ozkan, I. A.; Teja, A. S. *Fluid Phase Equilib.* **2005**, *228*, 487−491.
(17) Sanchez, I. C.; Lacombe, R. H. *Macromolecules* **1978**, *11*, 1145−1156.
(18) Doghieri, F.; Sarti, G. C. *J. Membr. Sci.* **1998**, *147*, 73−86.
(19) Giacinti Baschetti, M.; Doghieri, F.; Sarti, G. C. *Ind. Eng. Chem. Res.* **2001**, *40*, 3027−3037.

(20) Piccinini, E.; Giacinti Baschetti, M.; Sarti, G. C. *J. Membr. Sci.* **2004**, *234*, 95−100.
(21) Kang, Y. S.; Meldon, J. H.; Sung, N. H. *Polym. Eng. Sci.* **1986**, *25*, 1045−1049.
(22) Vogt, B. D.; Lin, E. K.; Wu, W.; White, C. C. *J. Phys. Chem. B* **2004**, *108*, 12685−12690.
(23) Yamamoto, Y.; Ferrari, M. C.; Giacinti Baschetti, M.; De Angelis, M. G.; Sarti, G. C. *Desalination* **2006**, *200*, 636−638.
(24) Catalano, J.; Myezwa, T.; De Angelis, M. G.; Giacinti Baschetti, M.; Sarti, G. C. *Int. J. Hydrogen Energy* **2012**, *37*, 6308−6316.
(25) Ferrari, M. C.; Galizia, M.; De Angelis, M. G.; Sarti, G. C. *Ind. Eng. Chem. Res.* **2010**, *49*, 11920−11935.
(26) Hallinan, D. T., Jr.; Elabd, Y. A. *J. Phys. Chem. B* **2009**, *113*, 4257−4266.
(27) Berens, A. R.; Hopfenberg, H. B. *Polymer* **1978**, *19*, 489−496.
(28) Dimos, V.; Sanopoulou, M. *J. Appl. Polym. Sci.* **2005**, *97*, 1184−1195.
(29) Du, A.; Koo, D.; Theryo, G.; Hillmyer, M. A.; Cairncross, R. A. *J. Membr. Sci.* **2012**, *396*, 50−56.
(30) Sarti, G. C.; Doghieri, F. *Chem. Eng. Sci.* **1998**, *53*, 3435−3447.
(31) Galizia, M.; De Angelis, M. G.; Sarti, G. C. *J. Membr. Sci.* **2012**, *405*−*406*, 201−211.
(32) De Angelis, M. G.; Sarti, G. C. *AIChE J.* **2012**, *58*, 292−301.
(33) *PvT* data for PLA. Nature Works PLA. Moldflow Materials Testing Report: MAT2238, http://www.natureworksllc.com/technical-resources/~/media/technical_resources/properties_documents/propertiesdocument_7000dmoldflowreport_pdf.pdf (accessed Sept 20, 2010).
(34) De Angelis, M. G.; Sarti, G. C.; Doghieri, F. *J. Membr. Sci.* **2007**, *289*, 106−122.
(35) Chapman, W. G.; Gubbins, K. E.; Jackson, G.; Radosz, M. *Fluid Phase Equilib.* **1989**, *52*, 31−38.
(36) Gross, J.; Sadowski, G. *Ind. Eng. Chem. Res.* **2001**, *40*, 1244−1260.
(37) Scatena, L. F.; Brown, M. G.; Richmond, G. L. *Science* **2001**, *292*, 908−912.
(38) Du, Q.; Superfine, R.; Freysz, E.; Shen, Y. R. *Phys. Rev. Lett.* **1993**, *70*, 2313−2316.
(39) Buck, U.; Huisken, F. *Chem. Rev.* **2000**, *100*, 3863−3890.
(40) Paul, J. B.; Collier, C. P.; Saykally, R. J.; Scherer, J. J.; O'Keefe, A. *J. Phys. Chem. A* **1997**, *101*, 5211−5214.
(41) Pérez, C.; Muckle, M. T.; Zaleski, D. P.; Seifert, N. A.; Temelso, B.; Shields, G. C.; Kisiel, Z.; Pate, B. H. *Science* **2012**, *336*, 897−901.